Am J Cancer Res 2023;13(7):2922-2937
www.ajcr.us /ISSN:2156-6976/ajcr0150357

Original Article

Indisulam exerts anticancer effects via modulation of transcription, translation and alternative splicing on human cervical cancer cells

Zhihui Dou[1,2,3,4], Xuetian Zhang[1,2,3,4], Wei Su[1,2,3,4], Taotao Zhang[1,2,3,4], Fei Ye[1,2,3,4], Dapeng Zhao[1,2,3,4], Xiaohua Chen[1,2,3,4], Qiang Li[1,2,3,4], Hong Zhang[1,2,3,4], Cuixia Di[1,2,3,4]

[1]Bio-Medical Research Center, Institute of Modern Physics, Chinese Academy of Sciences, Lanzhou 730000, Gansu, China; [2]Key Laboratory of Heavy Ion Radiation Biology and Medicine of Chinese Academy of Sciences, Lanzhou 730000, Gansu, China; [3]College of Life Sciences, University of Chinese Academy of Sciences, Beijing 100039, China; [4]School of Nuclear Science and Technology, University of Chinese Academy of Sciences, Beijing 100039, China

Received March 26, 2023; Accepted June 6, 2023; Epub July 15, 2023; Published July 30, 2023

Abstract: Indisulam is a synthetic sulfonamides drug with anticancer activity in various tumors. However, the effect and molecular mechanism of indisulam have still not been studied in human cervical cancer. We treated human cervical cancer cell lines (HeLa and C33A) with indisulam, evaluated its efficacy, and investigated its molecular targets. Indisulam inhibited tumor growth and induced RBM39 degradation in a dose-dependent manner. RNA-seq and proteomics analysis revealed that indisulam disrupted transcriptional regulation pathways related to mRNA splicing and apoptosis. More importantly, indisulam caused mis-splicing of RNA transcripts including p73 isoforms ΔNp73 and TAp73 which have opposite roles in apoptosis regulation. Indisulam increased TAp73 expression and triggered mitochondrial apoptosis independent of p53 status in HeLa cells. In summary, our data suggests that indisulam has therapeutic potential in cervical cancer, representing an attractive strategy in p53-disrupted cancers and should be further investigated.

Keywords: Indisulam, RBM39, splicing, p73, apoptosis

Introduction

Cervical cancer is one of the most common tumors of the female reproductive system and the fourth leading cause of death in women [1]. According to the *International Center for Research on Cancer*, approximately 485,000 cases of cervical cancer were diagnosed worldwide in 2013, resulting in 236,000 deaths [2]. Currently, the main treatment modalities for cervical cancer include surgery, chemotherapy, radiotherapy. However, the tolerance of radiotherapy and chemotherapy is still presents a major challenge, leading to poor treatment effects or failures in cervical cancer [3]. Therefore, identifying novel therapeutic agents is beneficial for improving the clinical management of cervical cancer.

In recent years, some new anti-cancer drugs have been derived from sulfonamides through anti-tumor screening and flow cytometry, such as indisulam (N-(3-chloro-7-indolyl)-1,4-benzenedisulfonamide; E7070) (**Figure 1A**) [4, 5]. Indisulam has exhibited potent anti-cancer activity against various tumor cell lines in vitro, including colorectal cancer cells HCT116 and SW620, non-small cell lung cancer cells LX-1 and PC-9 [6-9]. It can down-regulate genes involved in cell proliferation and tumor resistance and synergize with other anti-cancer drugs such as CPT-11 to exert anti-cancer effects [10]. Similarly, indisulam has shown an anti-tumor role in xenograft tumor models in vivo and induced tumor regression [11]. Moreover, indisulam can induce ubiquitination-mediated degradation of splicing factor RBM39 by recruiting it to DCAF15. This resulted in splicing defects, altered gene expression, and apoptosis of cancer cells [11]. Although the anti-cancer effect of indisulam has been reported, its role and mechanism in cervical cancer remain

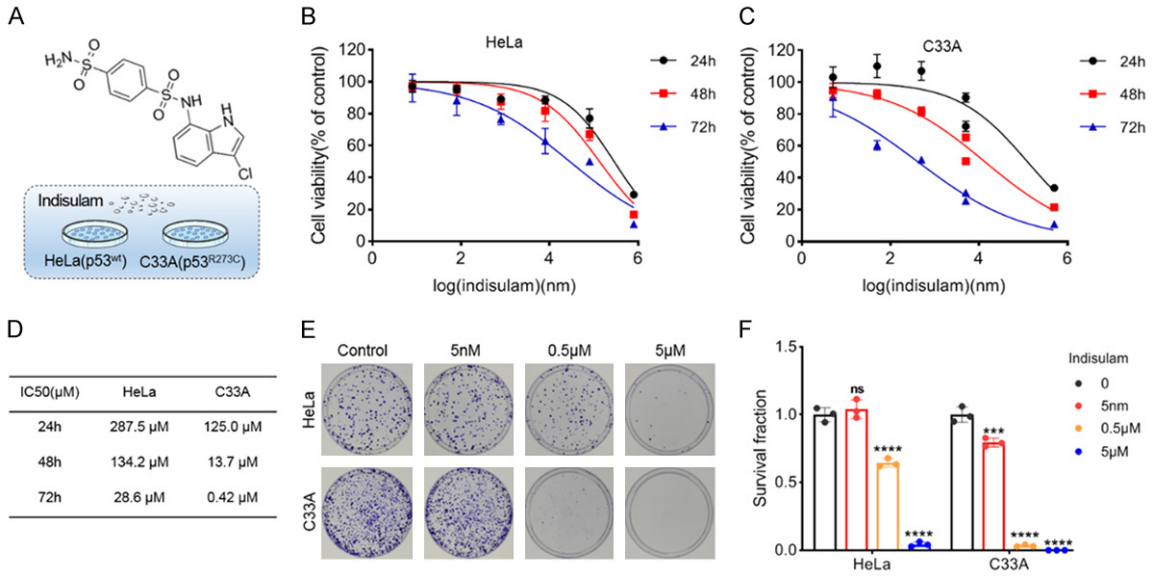

Figure 1. Indisulam efficiently inhibits the growth and clone formation of cervical cancer cells. A. Chemical-structure of indisulam. B-D. HeLa and C33A cells were treated with increasing doses of indisulam for 24, 48, and 72 hours. After incubation time, cell viability assay (MTS) was performed. E, F. Clonogenic survival assay of HeLa and C33A cells after exposure to different doses of indisulam (0-5 μM). After 10-14 days, colonies greater than 50 cells were counted. Data represent the mean ± SD of three independent experiments each conducted in triplicate. ns: no significance difference, ***P<0.001, ****P<0.0001.

largely unexplored. Therefore, this study primarily aims to investigate the effect of indisulam on cervical cancer cells and its possible mechanism.

Materials and methods

Cell culture and reagents

The human cervical adenocarcinoma cell line HeLa (HPV-18 positive) and the cervical squamous cell carcinoma cell line C33A (HPV negative) were obtained from Shanghai Fuheng Biotechnology Co., Ltd. HeLa cells have wild-type p53, while C33A cells harbor a mutant p53 (R273C). Both cell lines were cultured at 37°C and 5% CO_2 in Dulbecco's modified Eagle's medium (DMEM) supplemented with 10% FBS (BI), penicillin (100 units/ml), and streptomycin (100 mg/ml). Purified indiulam (≥98%) (SML1225) was obtained from Sigma-Aldrich (Shanghai) Trading Co., Ltd. The chemical structure is shown in **Figure 1A**. Dimethylsulphoxide (DMSO) purchased from Solarbio Science & Technology Co., Ltd. was used to dissolve the drug into 20 mM stock solution.

Cell viability assay

The methy-l tetrazolium salt (MTS) assay was used to detect cell survival. HeLa and C33A cells were seeded at 3000 cells/well in 96-well plates and treated with various concentrations of indiulam. After 24 h, 48 h and 72 h of incubation, the Cell Titer 96 AQueous One Solution Cell Proliferation Assay (Promega, Beijing, China) was added to each well and incubated for another 60 min at 37°C. The absorbance at 490 nm was measured by a microplate spectrophotometer reader (Thermal Lab System, Finland), and normalized to the control for cell survival.

Clonogenic assay

The colony-formation assay was used to evaluate cell proliferation. HeLa and C33A cells were seeded at 1000 cells/dish in 60 mm dishes in triplicate and treated with different concentrations of indiulam. The cells were incubated at 37°C for 2 weeks and then fixed with 4% paraformaldehyde for 15 minutes. The colonies were stained with crystal violet, imaged and counted.

Cell apoptosis assay

Cell death was assessed by flow cytometry using the Annexin V-FITC Apoptosis Detection Kit I (BD, USA). The cells were harvested and washed twice with PBS after 24 hours of incubation at 37°C. Then they were resuspended in

75 μL of binding buffer and stained with 2.5 μL of Annexin V and 2.5 μL of propidium iodide (Annexin V-FITC Apoptosis Detection Kit I, BD, USA) in the dark. The samples were analyzed by a FlowSight flow cytometer (Amnis, Seattle, WA, USA) with IDEAS Application v6.0 software after 15 min of incubation in the dark.

Western blot analysis

HeLa cells were treated with various concentrations of indiulam at 37°C for 24 hours, and then the protein was extracted through adding the RIPA lysis buffer (Solarbio, China). The proteins were separated by SDS-PAGE according to their molecular weight and then transferred to PVDF membranes activated by methanol. The membranes were blocked with 5% skim milk for 1 h and then incubated with antibodies against RBM39 (Abcam, ab244254, 1:1000), caspase-3 (Abcam, ab184787, 1:2000), ΔNp73 (Novus, 38C674.2, 1:1000), p73 (Novus, 5B-429, 1:1000), Cytochrome C (Immunoway, YM3402, 1:1000), Bax (Immunoway, YT0455, 1:1000), Bcl-2 (Immunoway, YT0470, 1:1000), Cleaved Caspase-3 (Cell Signaling Technology, 9661S, 1:1000), p21 (Abcam, ab109199, 1:1000), Cyclin D1 (Abcam, ab16663, 1:200), and β-Actin (Bioss, bs-10966R, 1:5000). The secondary antibodies were HRP-linked anti-mouse or anti-rabbit IgG antibodies (Bioss, 1:10000, China). The signals were detected by enhanced chemiluminescence.

RNA sequencing and proteome analysis

RNA sequencing: Human cervical cancer HeLa cells were treated with or without 5 μM indiuslam for 24 h. The cells were trypsinized and washed thoroughly with sterile PBS, and then fully lysed with Trizol. Total RNA was then isolated and purified. The isolated RNA has integrity greater than 7.0, and a yield greater than 1 μg. Oligo dT beads were used to interact with the ploy(A) tail of mature mRNA to eliminate other RNA, and then the purified mRNA was fragmented using a magnesium disruption kit. The cDNA was synthesized from mRNA by reverse transcriptase. Then the second strand was synthesized and the mRNA was removed to obtain double-stranded cDNA, which was purified. Then PCR amplification was performed to form a 300±50 bp fragment size library. After amplification, the library was purified and subjected to quality inspection. Finally, paired-end sequencing was performed using an illumina Novaseq™ 6000 following standard procedures in PE150 mode. After sequencing, the data was processed to remove the adapter, and the quality was evaluated. After alignment with the reference sequence, the differential gene expression analysis and transcript information were further analyzed.

Proteome analysis: Human cervical cancer HeLa cells were treated with or without 5 μM indiuslam for 24 h. Then cells were washed twice with sterile PBS, and then placed on ice. Sterile PBS pre-cooled at 4°C was added to the dishes. The cells were quickly scraped to the side of the dish with a cell scraper, and the cell lysates were collected and centrifuged. Protein samples were extracted, quantified and subjected to SDS-PAGE gel electrophoresis and FASP enzyme digestion. Then 100 μg of each group of samples were labeled with TMT, and the labeled peptides were mixed. The Agilent 1260 infinity II HPLC system was used for classification, and finally the peptides were identified by Easy nLC chromatography and mass spectrometry. The mass number deviation of the peptides was determined by database comparison, and the bioinformatics analysis was performed. Total RNA was isolated using TRIzol reagent (Invitrogen, CA, USA). Then, we performed paired-end sequencing on an Illumina Hi Seq 4000 at LC-BIO Technologies (Hangzhou) Co., LTD., following the vendor's recommended protocol.

Alternative splicing analysis

The predicted gene model (transcript.gtf) from Stringtie was used to qualitatively analyze the alternative splicing events for each sample using ASprofile software. The analysis of alternative splicing events was based on the gene structure annotation information of the species. The main types of variable splicing events are as follows: (A) exon skipping (SKIP) and cassette exons (MSKIP); (B) retention of single (IR) and multiple (MIR) introns; (C) alternative exon ends (AE); (D) alternative transcription start site (TSS); (E) alternative transcription termination site (TTS).

Immunofluorescence staining of nuclear speckles

HeLa cells treated with or without indisulam were grown on U20 mm glass-bottom cell cul-

ture dishes and fixed with 4% fixative solution. Then they were permeabilized with 0.5% Triton X-100 and blocked with 10% BSA in TBST. Next, the cells were incubated overnight at 4°C with primary antibodies against SC35 (ab11826, 1:200, Abcam) and Lamin A (ab8090, 1:1000, Abcam). Finally, they were incubated with secondary antibody in the dark for 1 h at room temperature. Cell images were acquired using a Zeiss LSM-700 confocal microscope (Carl Zeiss, Jena, Germany) (400×). Nuclear speckles are characterized by punctate immunofluorescence staining of the monoclonal antibody SC35-positive [12]. Lamin A was used to label the nuclear envelope.

Immunohistochemical (IHC)

The tumor tissues from xenograft tumors were subjected to IHC staining. Briefly, the tissue slides were dewaxed in xylene and rehydrated using different ethanol concentrations. Antigen retrieval was performed in sodium citrate buffer (10 mM, pH 6.0), followed by incubation with 3% H_2O_2 in methanol to block endogenous peroxidase. After incubated in blocking solution, slides were stained with Ki67 (Immunoway, YM3064, 1:200) primary antibodies overnight at 4°C. Finally, tumor slides were counterstained using hematoxylin.

Xenograft assay

Cervical cancer HeLa cells ($5*10^7$ cells in 1.25 mL serum-free medium) were injected into the axilla of the right forelimb of Balb/c nude mice (100 μL/each mice). After the injection, the mice were observed and then returned to the cage. When tumors grew to about 100 mm^3, the nude mice were randomly divided into three groups: the control group, the vector group (injected with the same volume of solvent) and drug treatment group (injected with 25 mg/kg indisulam), with 4 mice in each group. The mice were treated by tail vein injection once a day for 8 consecutive days. The body weight and tumor volume of nude mice were measured every 2 days and tumor volume was calculated as (length × $width^2$)/2. After discontinuing the drug administration, the nude mice were anesthetized, and the tumor tissues were collected, photographed, weighed.

Statistical analysis

Statistical analysis was performed using GraphPad Prism 8. The data were obtained from at least three independent experiments and presented as mean ± SD. T-Test and one-way ANOVA were used to determine the significance of differences between groups. A p-value <0.05 was considered statistically significant.

Results

Indisulam causes growth inhibition in a time and dose-dependent manner

We first investigated the cytotoxicity and inhibitory effects of indisulam on human cervical cancer cells. HeLa and C33A cells were treated with increasing concentrations of indisulam for 24-72 hours and then assessed by MTS assay. The result showed that indisulam significantly reduced the growth and viability of HeLa and C33A cells in a time- and dose-dependent manner (**Figure 1B**, **1C**). The half-maximal inhibitory concentration (IC50) was 287.5 μM in HeLa cells and 125.0 μM in C33A cells at 24 hours (**Figure 1D**). Moreover, we performed a colony-formation assay to determine the antiproliferative effect of indisulam. Our data suggested that indisulam treatment markedly decreased the clonogenicity of HeLa and C33A cells (**Figure 1E**, **1F**), indicating that indisulam suppressed the proliferation of cervical cancer cells.

Indisulam treatment inhibited cervical cancer in vivo

We further evaluated whether the same inhibition phenomenon could be observed in vivo using a nude mice model. Our results showed that compared with the control group, the tumor volume of nude mice treated with 25 mg/kg indisulam was significantly reduced (**Figure 2A**, **2B**). The weight of tumors in the indisulam treatment group was lower than those in the control and vehicle group (**Figure 2C**). Then, we performed histological analysis (HE, and Ki-67) staining to further assess the anti-tumor ability of indisulam in vivo. H&E staining of the tumor histopathology showed that tumor cell proliferation was significantly decreased in the indisulam treated group (**Figure 2D**). Consistently, the IHC results showed that the population of Ki67-positive cells was noticeably decreased in indisulam treated cells compared with control group (**Figure 2D**). This suggests that indisulam also has an antitumor effect in human cervical cancer HeLa cell xenograft tumor model.

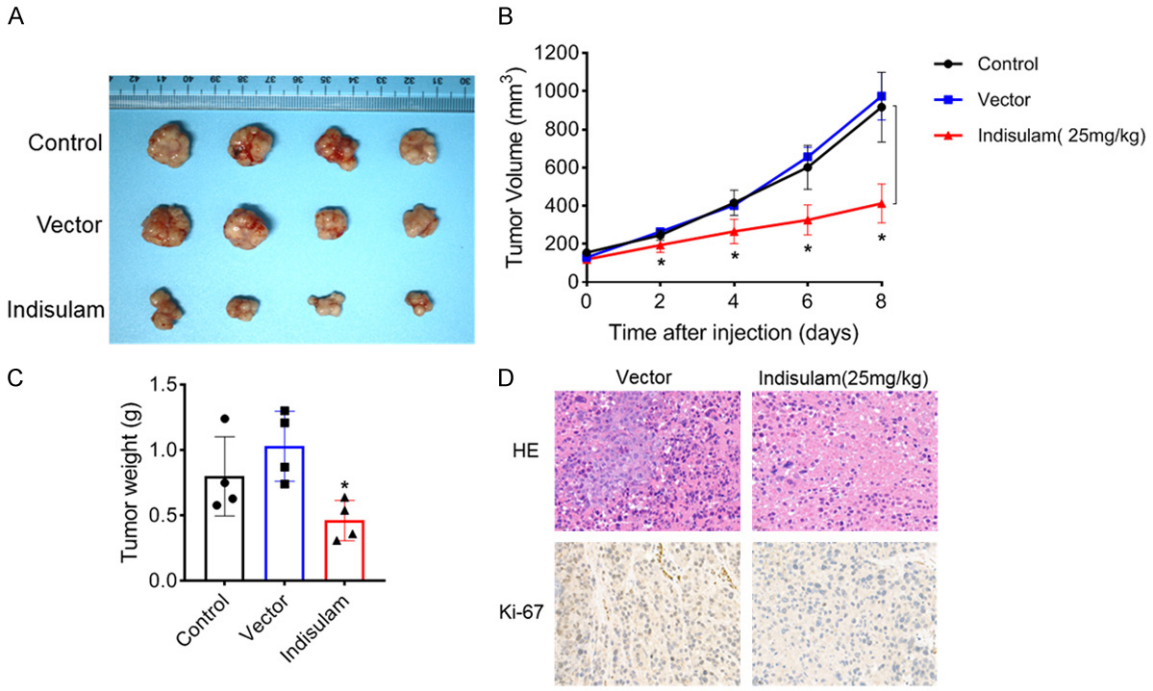

Figure 2. Indisulam suppressed tumorigenicity in *vivo*. A. Representative picture showing tumor growth after tail vein injection once a day for 8 consecutive days. B. Tumors' volume was measured on day 0, 2, 4, 6, 8. The weight of control, vector and indisulam-group tumors were measured respectively (n=4). C. The weight of vector-group and indisulam-group tumors were measured respectively (n=4, one-way ANOVA). D. Representative images of H&E staining and Ki-67 expression was assessed in xenografts. All statistical data were shown as mean ± SEM. **P*<0.05.

Indisulam-treatment could cause a depletion of RBM39 in HeLa cell

The precise molecular mechanism of indisulam has been recently elucidated. Indisulam acts as "molecular glue" that recruits splicing factor RBM39 to the E3 ubiquitin ligase CRL4-DCAF15, leading to rapid proteasomal degradation of RBM39 (**Figure 3A**) [13, 14]. Indisulam binds to a well-defined pocket formed by DCAF15 and establishes several direct and water-mediated interactions with both RBM39 and DCAF15 [15] (**Figure 3B**). To investigate whether indisulam could also induce RBM39 degradation in cervical cancer cells, we performed transcriptome and proteomic analysis on HeLa cells treated with indisulam (5 μM) for 24 hours. Heatmap analysis showed no decrease in RBM39 mRNA level, but a significant down-regulation of RBM39 protein in indisulam-treated HeLa cells was observed (**Figures 3C**, **4A**), indicating that the reduction in RBM39 expression was post-translational. The dose-dependent degradation of RBM39 was also confirmed by western blot in HeLa and C33A cells treated with indisulam (**Figure 3D**, Supplementary Figure 1). In addition, expression-level modification of some ubiquitin pathway-related proteins, such as DCAF, DDB2, UBE2D4, etc., were also detected in our sequencing results. Together, these results show that indisulam treatment can reduce RBM39 protein levels in cervical cancer cells.

Transcription perturbations following indisulam treatment in HeLa cells

We performed total RNA-seq on HeLa cells to identify transcriptional changes caused by RBM39 degradation induced by indisulam treatment. RBM39 selectively coactivates components of well-known transcription factor involved in multiple cellular activities, such as AP-1, steroid hormone receptors including ERα, ERβ and PR, and NF-κB et al. [16]. However, RBM39 also appears to act as a transcription corepressor. Kumar et al. revealed that RBM39 could interact with TBX3 to suppress the expression of the lncRNA UCA1 and prevent cell senescence [17]. RBM39-knockdown has been shown to result in the up- or down-regula-

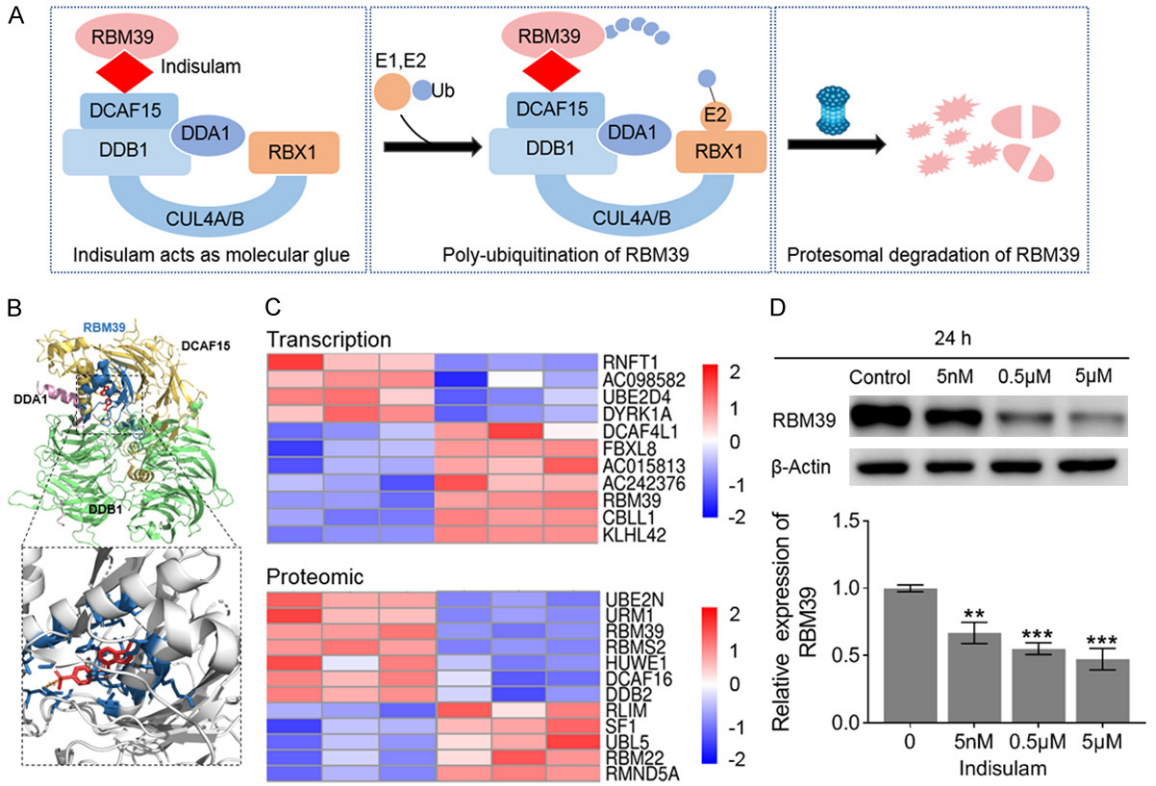

Figure 3. Indisulam treatment induces RBM39 degradation of HeLa cells. A. Indisulam act as a molecular glue recruiting RBM39 to E3 ubiquitin ligase CRL4-DCAF15 resulting in proteasomal degradation of RBM39. B. Structural of indisulam-mediated RBM39 recruitment to DCAF15 E3 ligase complex. C. Heatmap analysis following indisulam treatment in HeLa cells after 24 h treatment (5 μM). D. Western blot of HeLa cells treated with 0, 5 nM, 0.5 μM or 5 μM indisulam for 24 h. Data represent the mean ± SD of three independent experiments each conducted in triplicate. ***P*<0.01, ****P*<0.001, *****P*<0.0001 (one-way ANOVA).

tion of transcript levels of various genes [18]. We filtered the differentially expressed genes (DEGs) with a fold change (FC) ≥2 or ≤0.5 and *p* value <0.05. FPKM was used to evaluate gene expression level across different samples. The result showed that indisulam treatment significantly perturbed 256 DEGs: 180 were up-regulated and 76 were down-regulated (**Figure 4A**, **4B**), suggesting that indisulam treatment can both increase and decrease the transcript levels. These DEGs participate in various cellular processes such as transcription regulation, mRNA splicing, post-translational protein modification, cell cycle arrest and apoptosis (**Figure 4C**). KEGG pathway analysis showed that the DEGs were predominately enriched in transcriptional mis-regulation and cancer-associated pathways (**Figure 4D**). Collectively, these results indicate that indisulam-induced RBM39 degradation results in transcription perturbations of HeLa cells in multiple cellular processes.

Translation perturbations following indisulam treatment in HeLa cells

RBM39 has been demonstrated to regulate protein translation and bind to mRNAs encoding translation-related proteins [18]. In addition, Mai et al. found that RBM39 binds to 5'UTR, affecting protein translation [4]. To investigate how indisulam affects protein expression in HeLa cells, we performed a proteomic analysis following RBM39 depletion by indisulam. Quantification of SDS-PAGE results confirmed protein quality, quantity, and sample repeatability. Peptide labeling efficiency was 99.2%, enabling subsequent analysis. We used a fold change (FC) of >1.2 and a *p* value of <0.05 as criteria for selecting differential proteins. Interestingly, we identified 479 differential proteins, of which 340 were up-regulated and 139 were down-regulated. Notably, RBM39 levels were significantly down-regulated (**Figure 5A**, **5B**). According to the subcellular localiza-

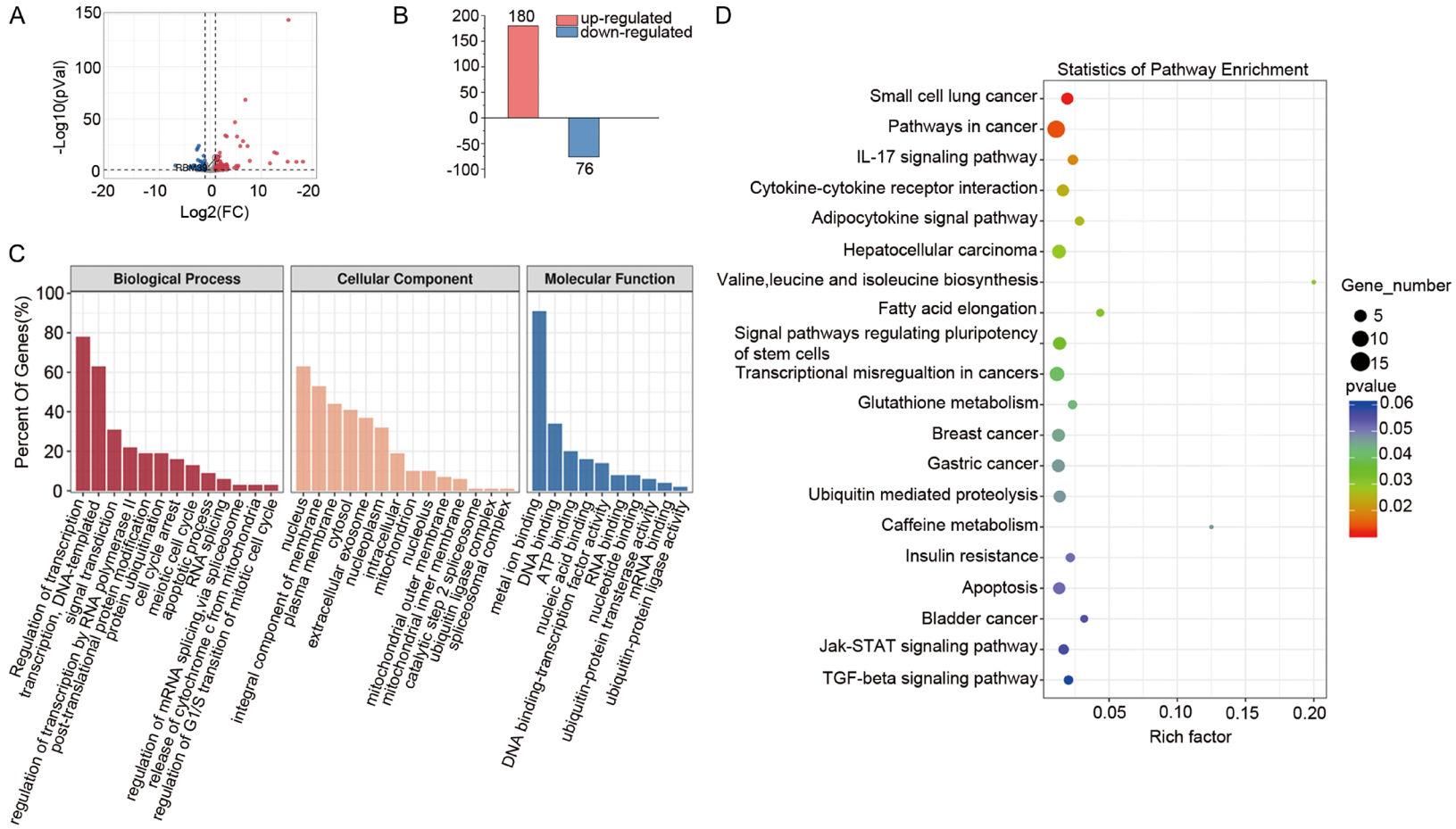

Figure 4. Indisulam regulates transcript levels. A. Volcano plot of transcriptional analysis in HeLa cells treated with 5 μM indisulam for 24 h. B. The Bar graph of up-regulated and down-regulated DEGs. DEGs were defined as genes with a FC≥2 or ≤0.5 and *p* value <0.05. C. The significantly enriched GO terms influenced by indisulam are shown here. D. The KEGG enrichment analysis of HeLa cells influenced by indisulam.

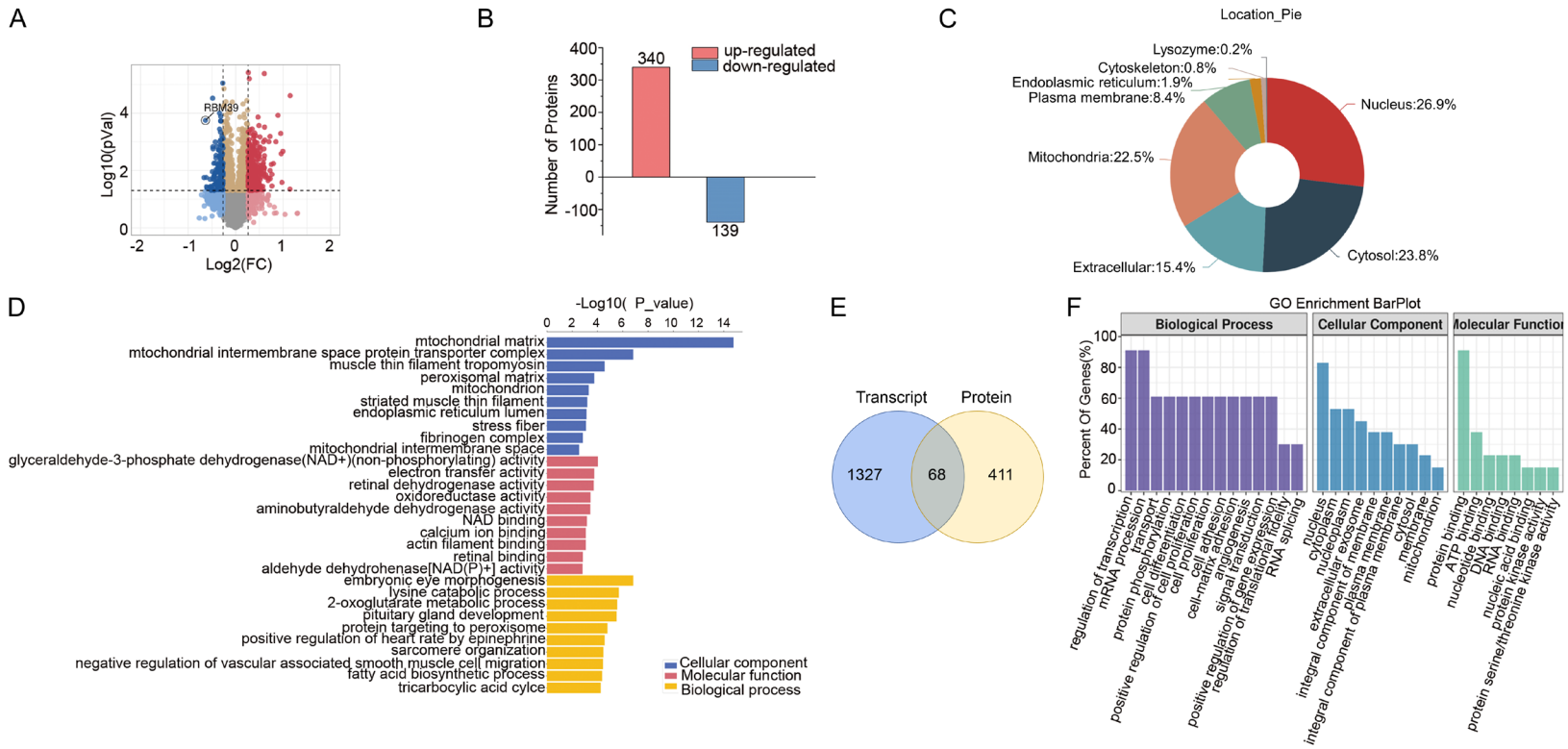

Figure 5. Indisulam regulates translation levels. A. Volcano plot of proteomic analyses in HeLa cells treated with 5 μM indisulam for 24 h. B. The Bar graph of up-regulated and down-regulated proteins were defined as genes with a FC≥1.2 or ≤0.5 and *p* value <0.05. C. Pie chart of differential proteins subcellular localization. D. Bar plot showing the dysregulated GO terms. E. Venn plot of integrated transcriptomic and proteomic analyses. F. Enriched GO terms analysis of 68 genes in common influenced by indisulam.

tion analysis, we found that most differential proteins were located in the nucleus and cytoplasm, while about 22.5% were located in the mitochondria (**Figure 5C**). Gene ontology (GO) enrichment analysis highlighted the involvement of differential proteins in mitochondrial matrix functions (**Figure 5D**), suggesting that mitochondrial pathways may be important for HeLa cells' response to indisulam. Furthermore, we integrated transcriptomic and proteomic analyses and found about 68 genes that showed consistent changes at both mRNA and protein levels (**Figure 5E**). Enrichment analysis revealed that processes associated with transcription regulation, mRNA splicing, protein modification and cell proliferation or differentiation were particularly impacted (**Figure 5F**). These processes are crucial for events occurring in the nucleus, cytoplasm, and mitochondria, implying that HeLa cells undergo multiple changes following indisulam treatment.

Indisulam treatment is associated with defects in RNA splicing in HeLa cells

Han T et al. demonstrated that indisulam toxicity is caused by RBM39-dependent splicing disturbance and aberrant splicing events [13]. In our study, we performed alternative splicing analysis using reads uniquely mapped to the human genome and identified 6063 RBM39-regulated events. The most common event was exon skipping (2054/6063, 33.9%), followed by alternative transcription start site (1448/6063, 23.9%) and alternative transcription termination site (756/6063, 12.5%) (**Figure 6A**). We additionally observed intron retention (543/6063, 8.9%) and alternative 3'/5' splicing sites (750/6063, 12.4%). By intersecting a dataset of splicing factors (SFs) [19] with differentially expressed genes (DEGs), we identified 7 SFs that were differentially expressed at the proteome level, with six of them having direct or indirect interaction with RBM39 (**Figure 6B**). We also found a strong correlation between RBM39 expression and other DSFs in CESC samples (TIMER2.0) (**Figure 6C**), suggesting RBM39 may regulate multiple splicing factors and splicing events in CESC.

To investigate the impact of splicing disruption on nuclear speckle organization after indisulam treatment, we used an antibody against splicing factor SC35 to label nuclear speckles in HeLa cells. SC35 is a marker of nuclear speckles where splicing and transcription factors are abundant [19, 20]. As expected, indisulam treatment resulted in larger, rounder, fewer and brighter speckles compared to control group (**Figure 6D**), which are referred to as mega-speckles. We observed minimal colocalization of RBM39 and SC35, indicating a negative correlation between RBM39 levels and the formation of SC35 speckles (**Figure 6E**). The results suggested that indisulam treatment disrupts the alternative splicing leading to the reorganization of splicing factors into larger and rounder granule clusters within the nucleus of HeLa cells.

Indisulam induces mitochondrial apoptosis independently of p53 in HeLa cells by redirecting p73 alternative splicing

We performed an Annexin V-FITC dual staining assay by flow cytometry to investigate the effect of indisulam on apoptosis in HeLa cells. Our findings revealed an increase in apoptotic cells with higher concentrations of indisulam (**Figure 7A**), suggesting that indisulam might inhibit cancer growth by inducing cell apoptosis. Since p53 is inactivated in HPV-18 positive HeLa cells, and p73 can induce apoptosis independently of p53 by regulating genes involved in apoptosis in many cancers, we examined whether p73 mediates indisulam-induced apoptosis in HeLa cells. p73 has two splicing isomers with opposite functions: anti-apoptotic factor ΔNp73 and pro-apoptotic factor TAp73. The regulation of p53 responsive genes in the absence of p53 relies on a critical balance between different p73 gene-derived proteins [21]. Our results showed that indisulam treatment reduced ΔNp73 expression but increased TAp73 expression, indicating that indisulam might modulate apoptosis in HeLa cells by altering the alternative splicing of apoptotic factors and changing the ΔNp73/TAp73 ratio (**Figure 7B**, **7C**). To further confirm intrinsic apoptosis induced by indisulam treatment in HeLa cells, we performed western blot assay to detect the mitochondrial pathway-related proteins. As shown in **Figure 7D** and **7E**, indisulam treatment upregulated the expression of pro-apoptotic Bax and decreased the anti-apoptotic Bcl-2 expression, resulting in an increase in the ratio of Bax/Bcl-2, promoting cell apopto-

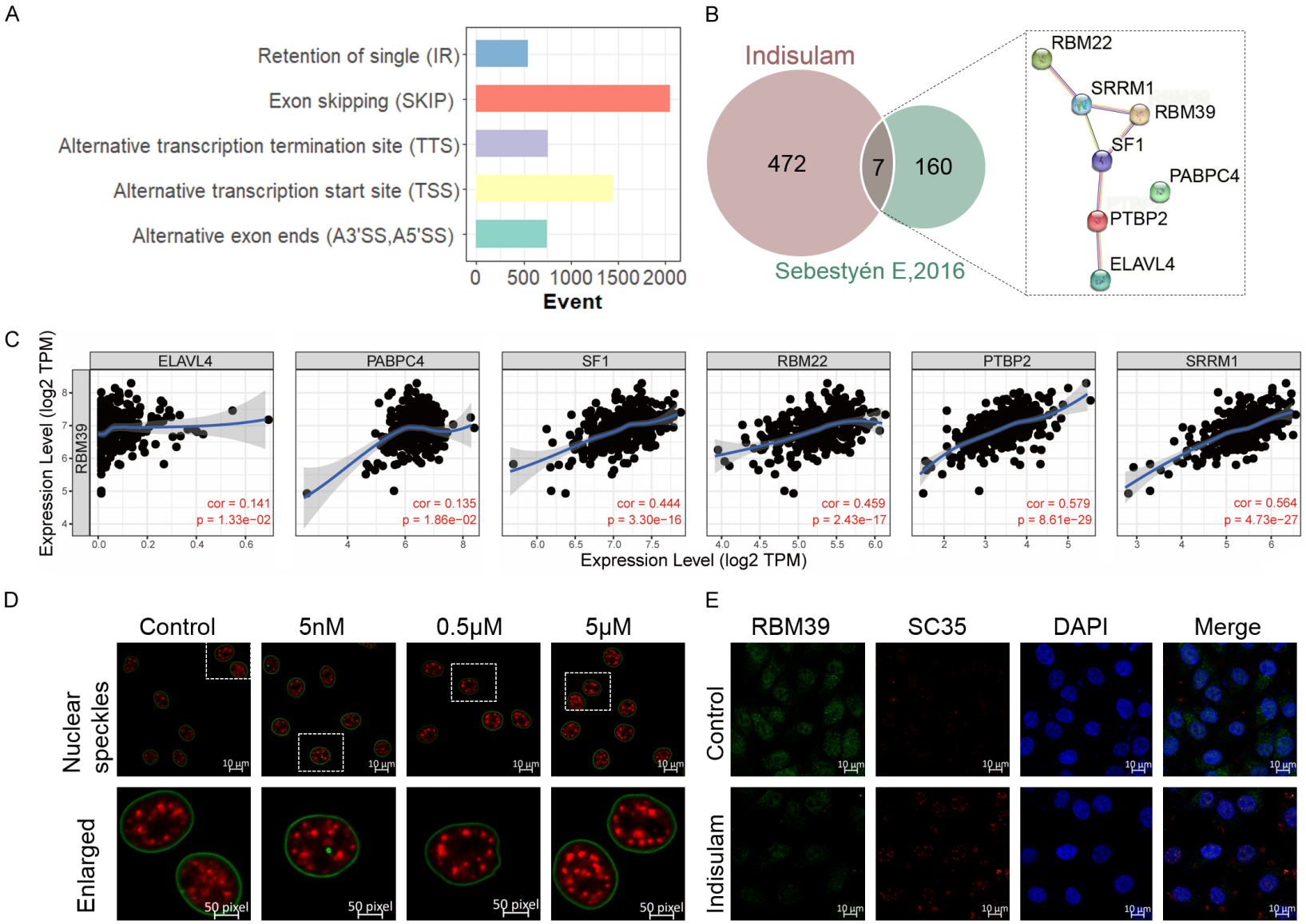

Figure 6. Indisulam treatment causes mis-splicing of RNA in HeLa cells. A. Number of RNA splicing events (ASprofile, n=3 independent experiments) in HeLa cells following treatment with 5 μM indisulam for 24 h. B. Venn plot of differentially expressed alternative splicing factors at protein level and protein-protein interacting network between differentially expressed splicing factors and RBM39. C. Analysis of correlation between differentially expressed splicing factors and RBM39 expression by using TIMER database in CESC. D. Morphologic change of nuclear speckles in HeLa cells after indisulam treatment for 24 h. Nuclear speckles were stained with anti-SC35 antibody (red); anti-lamin A antibody (green) was used to stain nuclear membrane. E. Colocalization analysis of RBM39 (green) and nuclear speckles (red) in HeLa cells after indisulam treatment for 24 h.

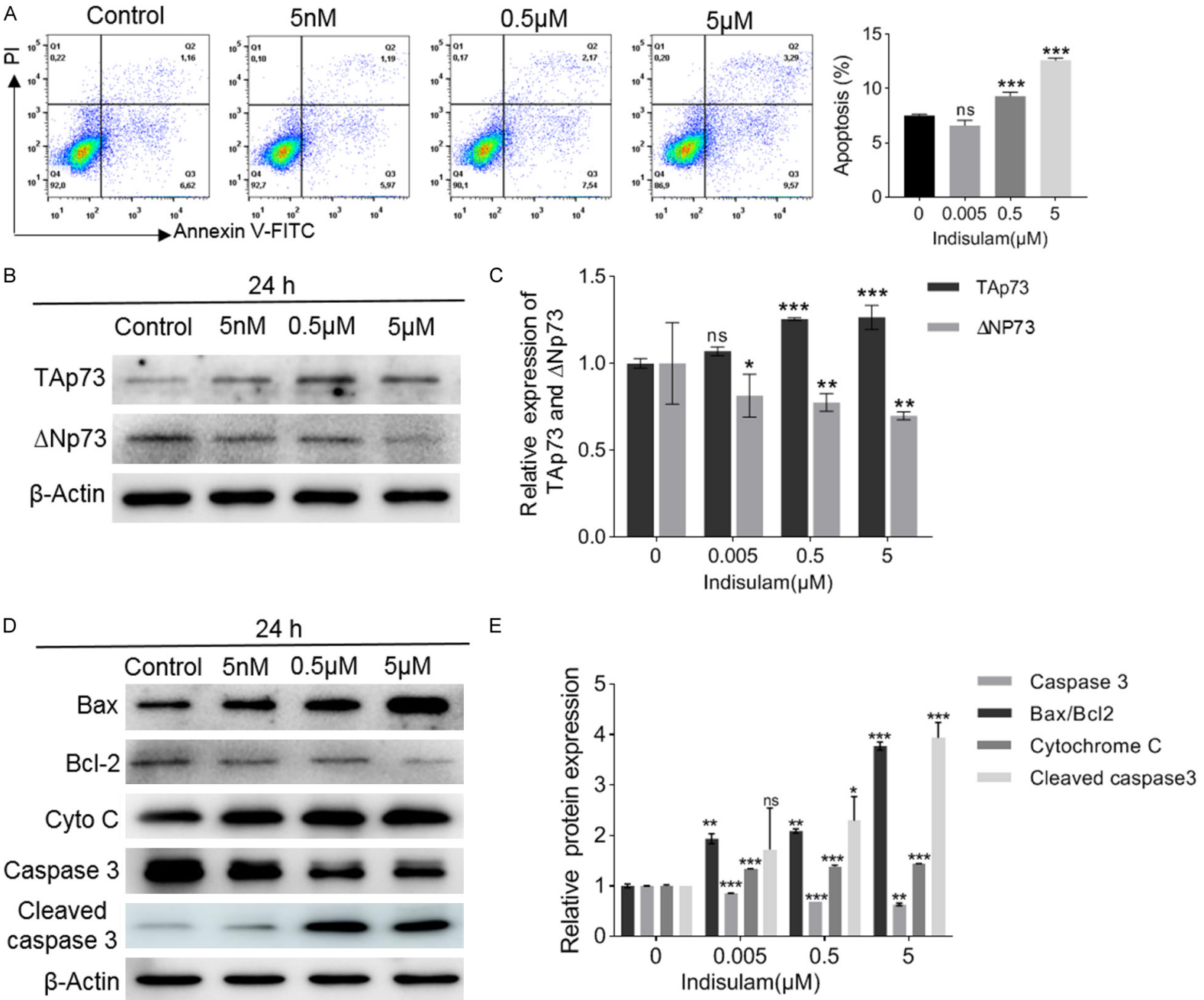
A
Control
5nM
0.5μM
5μM
PI
Annexin V-FITC
Q1 0,22
Q2 1,16
Q4 92,0
Q3 6,62
Q1 0,10
Q2 1,19
Q4 92,7
Q3 5,97
Q1 0,17
Q2 2,17
Q4 90,1
Q3 7,54
Q1 0,20
Q2 3,29
Q4 86,9
Q3 9,57
Apoptosis (%)
ns
***
***
***
0
5
10
15
0
0.005
0.5
5
Indisulam(μM)
B
24 h
Control
5nM
0.5μM
5μM
TAp73
ΔNp73
β-Actin
C
Relative expression of TAp73 and ΔNp73
TAp73
ΔNP73
ns
*
***
**
***
**
0.0
0.5
1.0
1.5
0
0.005
0.5
5
Indisulam(μM)
D
24 h
Control
5nM
0.5μM
5μM
Bax
Bcl-2
Cyto C
Caspase 3
Cleaved caspase 3
β-Actin
E
Relative protein expression
Caspase 3
Bax/Bcl2
Cytochrome C
Cleaved caspase3
0
1
2
3
4
5
0
0.005
0.5
5
Indisulam(μM)

Figure 7. Indisulam treatment induce p73-dependent mitochondrial pathway of apoptosis in HeLa cells. A. HeLa cells treated with different concentration of indisulam for 24 h were subsequently detected using co-staining with Annexin V-FITC and PI flow cytometry. B. Expression of p73 splicing isoforms ΔNp73 and TAp73 were analysed by western blot assay. β-Actin protein was used as an internal control. C. Quantitative analysis of the ΔNp73 and TAp73 is represented by column graphs. D. Expression of apoptosis-associated proteins, including Bcl-2, Bax, procaspase-3, cleaved caspase 3 and cytochrome c were analysed by western blot assay. β-Actin protein was used as an internal control. E. Quantitative analysis of the Bcl-2, Bax, procaspase-3, cleaved caspase 3 and cytochrome c proteins were represented by column graphs. Data represent the mean ± SD of three independent experiments each conducted in triplicate. ns: no significant difference, **P*<0.05, ***P*<0.01, ****P*<0.001, *****P*<0.0001 (One-way ANOVA).

sis. Caspase-3, a crucial cysteine-aspartic acid protease involved in cell apoptosis, is cleaved by initiator caspases such as caspase-8 or caspase-9 at the Asp175 residue. This cleavage leads to the removal of the prodomain and the formation of two heterodimers, p20 and p12 (cleaved caspase-3) [22-24]. In our study, we observed downregulation of procaspase-3 expression and upregulation of cleaved caspase-3 following 24 hours of indisulam treatment. Furthermore, the level of cytochrome c increased, indicating the occurrence of apoptosis. Therefore, our findings confirm that indisulam affects p73 splicing independently of p53 and induces intrinsic apoptosis by upregulating Bax/Bcl-2 ratio, cytochrome c release and activated-caspase-3.

Discussion

Indisulam is an aryl sulfonamide drug originally discovered by Eisai in a phenotypic screen for small molecules with anticancer activity [4, 25]. A number of studies have shown that multiple cancer cell lines and xenograft models are sensitive to indisulam treatment [26-29]. However, the efficacy of indisulam has not been tested in human cervical cancer cells. In this study, we have shown that indisulam is an extremely effective anti-cancer drug in human cervical cancer cells, reducing cellular growth in a time and dose-dependent manner. In addition, although both HeLa and C33A cell lines responded to indisulam treatment, the IC50 concentrations were quite different, leading us to hypothesize that differences in p53 status might lead to the different degree of response. Recent studies have shed light on the precise molecular mechanism of indisulam's action and selectivity [13, 14]. It has been reported that the anti-tumor effect of indisulam is dependent on RBM39, also known as HCC1 and CAPER or CAPERα, and that RBM39 mutations can induce resistance to indisulam, preventing the formation of the complex [13]. Indisulam induces the recruitment of RBM39 to the CUL4-DCAF15 E3 ubiquitin ligase, resulting in polyubiquitination and rapid proteasomal degradation [13, 14]. In our study, we observed a significant decrease in RBM39 expression through Western blot and proteomic analysis, indicating that the efficacy of indisulam in HeLa cells may depend on RBM39 degradation. It has been demonstrated that RBM39 is involved in the coactivation of well-known transcription factors involved in multiple cellular activities, such as oestrogen receptor-α, ERβ, progesterone receptor, activating protein-1, oestrogen-related receptor-α and NF-κB [16]. RBM39-knockdown has been shown to be involved in the up- or down-regulation of transcript levels of various genes, potentially impacting translation [18]. Here, we have shown that indisulam treatment caused broad perturbations in HeLa cells both at the transcript and translation level, particularly in the regulation of transcription, mRNA splicing, apoptosis, ubiquitin-mediated proteolysis, and mitochondrial-associated GO terms (**Figure 8**). These results underline the broad regulatory actions of indisulam on HeLa cells which may be mediated by RBM39 degradation.

It is now widely accepted that defects in alternative splicing represents an actionable cancer hallmark [30, 31]. Carcinogenic splicing results from either mutations in splicing-regulatory elements of cancer-related genes or from abnormal expression of SF [32, 33]. Using small molecules to block or degrade the SF and modulate cancer-specific splicing have provided novel therapeutic targets for oncology [33, 34]. At present, the mechanism of action of small molecule splicing regulators has been gradually elucidated. The first class, including E7107 and pladienolide B act directly on the spliceosomal component SF3B1. In addition, several small molecules, for example NB-506, inhibit the activity of splicing factors by targeting the regulatory kinases of SFs. Finally, a class of aryl

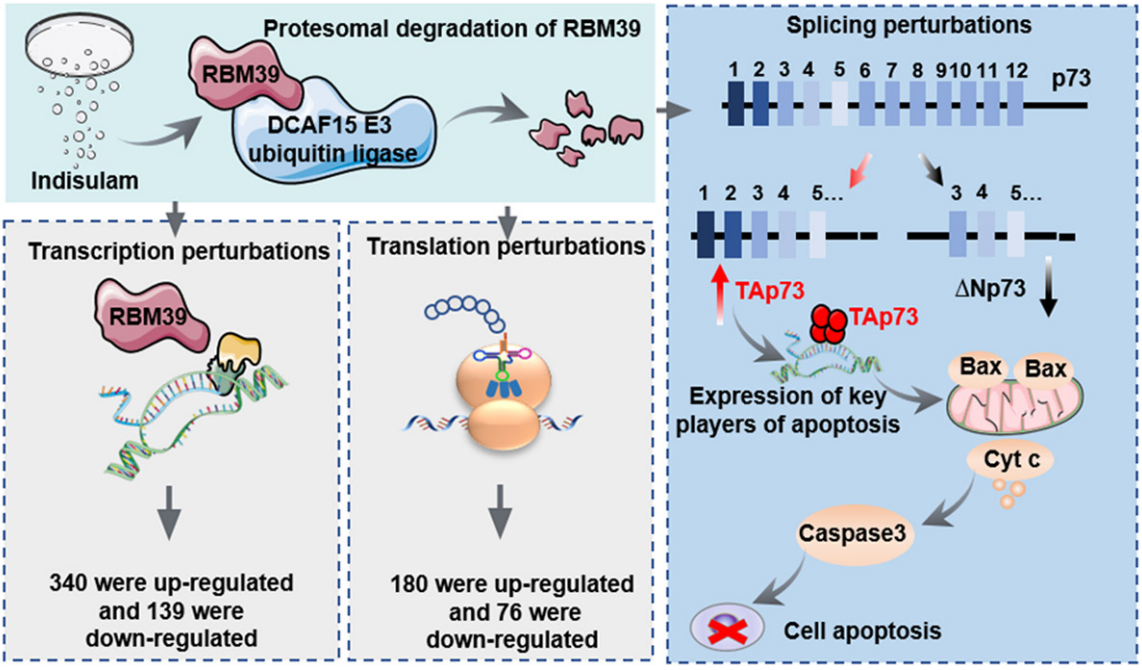

Figure 8. Model of potential targets of RBM39 in cancer. Indisulam treatment induced RBM39 degradation results in perturbations of transcription, translation and especially alternative splicing events in multiple cellular processes in HeLa cells. Surprisingly, indisulam treatment was able to alter the ΔNp73 to TAp73 ratio by redirecting the alternative splicing of p73 to induce mitochondrial apoptosis in HeLa cells independent of the P53 gene.

sulfonamides drug such as indisulam has been reported to achieve anti-cancer effect in multiple cancer types by decreasing the expression of RBM39 [13, 33]. RBM39 is associated with spliceosome component U2AF2 and multiple splicing factors. Ting Han et al. demonstrated that indisulam disrupts RBM39-dependent mRNA splicing, resulting in exon skipping and intron retention [13]. Recently, a study on neuroblastoma also reported that indisulam abrogates proteins involved in cell cycle and metabolism through RBM39-mediated alternative splicing. In our study, we also observed erroneous splicing of RNA and dysregulated expression and reorganization of splicing factor following indisulam treatment in HeLa cells. Aberrantly spliced genes and disregulated splicing factors might play an important role in cell apoptosis induction regulated by indisulam in human cervical cancer cells, which needs further exploration.

Our findings also highlight the ability of indisulam to induce apoptosis in HeLa cells in a time and dose-dependent manner. Apoptosis is a major mechanism of cancer cell death. Abnormalities in apoptosis play a crucial role in the progression and development of human cancer and targeting apoptosis has been a mainstay in cancer therapy [35]. There are two main established apoptotic signaling pathways in mammals: the extrinsic pathway of apoptosis mediated by death receptor and the intrinsic pathway of apoptosis mediated by mitochondria, also called mitochondrial apoptosis [36]. The extrinsic apoptotic signal is activated when extracellular death-inducing factors bind to cell receptors (TNFR, TRAIL, FasL), leading to the formation of death inducing signaling complexes. Diverse cellular stimuli including DNA damage, hypoxia and oxidative stress, activate the mitochondrial pathway of apoptosis by inducing oligomerization of Bax/Bak located in the mitochondrial outer membrane, promoting mitochondrial outer membrane permeability, the release of cytochrome c, and caspase activation [37]. All of these intrinsic apoptosis events are primarily controlled by Bcl-2 family proteins and p53 [38]. However, p53 is inactivated in HeLa cells because it is HPV-18 positive. It has been reported that p73, a homologue of the tumor suppressor factor p53, is a highly appealing therapeutic target towards cancers with a null or disrupted p53 pathway

[39]. Our previous study also found that p73 gene involved in the induction of mitochondrial apoptosis in HeLa cells by SF3B1 inhibition [40]. Due to the use of two alternative promoters, the TP73 gene results in the generation of TAp73 and ΔNp73 through alternative splicing [41]. The TAp73 isoforms act as tumor suppressors and have pro-apoptotic effects, whereas the ΔNp73 isoforms lack the N-terminus transactivation domain and act as oncogenes [42]. Herein, we showed that indisulam treatment could induce human cervical cancer cell apoptosis through regulating the alternative splicing of p73, favoring the splicing of pro-apoptotic splice variants TAp73 and further causing increased Bax expression and decreased Bcl-2. Additionally, activation of procaspase-3 and upregulation of cytochrome c was also observed, indicating that the apoptotic effects of indisulam against HeLa cells was modulated by p73/Bcl-2 protein-mediated regulation of mitochondrial apoptosis (**Figure 8**). However, whether indisulam treatment could also lead to other pathways of apoptosis through coordinating transcription, translation and alternative splicing is still unclear and needs to be explored in depth.

Altogether, this research indicates that indisulam treatment shows significant therapeutic potential as demonstrated by our results in HeLa cells by inducing proteasomal degradation of RBM39, transcription perturbations, mis-splicing, and p73-mediated mitochondrial apoptosis. With additional studies on the essential role of RBM39 as a target for cancer treatment, the efficacy of indisulam could be further optimized and could emerge as a promising drug candidate for the treatment of cervical cancer.

Acknowledgements

This work was supported by grants from the national Key R&D project of the Chinese Ministry of Science and Technology (2018-YFE0205100); the National Natural Science Foundation of China (11875299, 11675234); and Natural Science Foundation of Gansu Province, China (17JR5RA310).

Disclosure of conflict of interest

None.

Address correspondence to: Qiang Li, Cuixia Di and Hong Zhang, Department of Heavy Ion Radiation Medicine, Institute of Modern Physics, Chinese Academy of Sciences, Lanzhou 730000, Gansu, China. Tel: +86-931-496-9344; Fax: +86-931-496-9170; E-mail: liqiang@impcas.ac.cn (QL); dicx@impcas.ac.cn (CXD); zhangh@impcas.ac.cn (HZ)

References

[1] Liu M, Wang Z, Liu Q, Zhu H and Xu N. Expression of micro-RNA-492 (MiR-492) in human cervical cancer cell lines is upregulated by transfection with wild-type P53, irradiation, and 5-fluorouracil treatment in vitro. Med Sci Monit 2018; 24: 7750-7758.

[2] Global Burden of Disease Cancer Collaboration, Fitzmaurice C, Dicker D, Pain A, Hamavid H, Moradi-Lakeh M, MacIntyre MF, Allen C, Hansen G, Woodbrook R, Wolfe C, Hamadeh RR, Moore A, Werdecker A, Gessner BD, Te Ao B, McMahon B, Karimkhani C, Yu C, Cooke GS, Schwebel DC, Carpenter DO, Pereira DM, Nash D, Kazi DS, De Leo D, Plass D, Ukwaja KN, Thurston GD, Yun Jin K, Simard EP, Mills E, Park EK, Catalá-López F, deVeber G, Gotay C, Khan G, Hosgood HD 3rd, Santos IS, Leasher JL, Singh J, Leigh J, Jonas JB, Sanabria J, Beardsley J, Jacobsen KH, Takahashi K, Franklin RC, Ronfani L, Montico M, Naldi L, Tonelli M, Geleijnse J, Petzold M, Shrime MG, Younis M, Yonemoto N, Breitborde N, Yip P, Pourmalek F, Lotufo PA, Esteghamati A, Hankey GJ, Ali R, Lunevicius R, Malekzadeh R, Dellavalle R, Weintraub R, Lucas R, Hay R, Rojas-Rueda D, Westerman R, Sepanlou SG, Nolte S, Patten S, Weichenthal S, Abera SF, Fereshtehnejad SM, Shiue I, Driscoll T, Vasankari T, Alsharif U, Rahimi-Movaghar V, Vlassov VV, Marcenes WS, Mekonnen W, Melaku YA, Yano Y, Artaman A, Campos I, MacLachlan J, Mueller U, Kim D, Trillini M, Eshrati B, Williams HC, Shibuya K, Dandona R, Murthy K, Cowie B, Amare AT, Antonio CA, Castañeda-Orjuela C, van Gool CH, Violante F, Oh IH, Deribe K, Soreide K, Knibbs L, Kereselidze M, Green M, Cardenas R, Roy N, Tillmann T, Li Y, Krueger H, Monasta L, Dey S, Sheikhbahaei S, Hafezi-Nejad N, Kumar GA, Sreeramareddy CT, Dandona L, Wang H, Vollset SE, Mokdad A, Salomon JA, Lozano R, Vos T, Forouzanfar M, Lopez A, Murray C and Naghavi M. The global burden of cancer 2013. JAMA Oncol 2015; 1: 505-527.

[3] Huang SS, Hao DZ, Zhang Y, Liu HM and Shan WS. Progress in studies of the mechanisms and clinical diagnosis of cervical carcinoma associated with genomic integration of high-risk human papillomavirus DNA. Yi Chuan 2017; 39: 775-783.

[4] Owa T, Yoshino H, Okauchi T, Yoshimatsu K, Ozawa Y, Sugi NH, Nagasu T, Koyanagi N and Kitoh K. Discovery of novel antitumor sulfonamides targeting G1 phase of the cell cycle. J Med Chem 1999; 42: 3789-3799.

[5] Owa T, Yoshino H, Okauchi T, Okabe T, Ozawa Y, Hata Sugi N, Yoshimatsu K, Nagasu T, Koyanagi N and Kitoh K. Synthesis and biological evaluation of N-(7-indolyl)-3-pyridinesulfonamide derivatives as potent antitumor agents. Bioorg Med Chem Lett 2002; 12: 2097-2100.

[6] Supuran CT. Indisulam: an anticancer sulfonamide in clinical development. Expert Opin Investig Drugs 2003; 12: 283-287.

[7] Van Kesteren C, Beijnen JH and Schellens JH. E7070: a novel synthetic sulfonamide targeting the cell cycle progression for the treatment of cancer. Anticancer Drugs 2002; 13: 989-997.

[8] Punt CJ, Fumoleau P, van de Walle B, Faber MN, Ravic M and Campone M. Phase I and pharmacokinetic study of E7070, a novel sulfonamide, given at a daily times five schedule in patients with solid tumors. A study by the EORTC-early clinical studies group (ECSG). Ann Oncol 2001; 12: 1289-1293.

[9] Raymond E, ten Bokkel Huinink WW, Taïeb J, Beijnen JH, Faivre S, Wanders J, Ravic M, Fumoleau P, Armand JP and Schellens JH; European Organization for the Research and Treatment of Cancer Early Clinical Study Group. Phase I and pharmacokinetic study of E7070, a novel chloroindolyl sulfonamide cell-cycle inhibitor, administered as a one-hour infusion every three weeks in patients with advanced cancer. J Clin Oncol 2002; 20: 3508-3521.

[10] Ozawa Y, Kusano K, Owa T, Yokoi A, Asada M and Yoshimatsu K. Therapeutic potential and molecular mechanism of a novel sulfonamide anticancer drug, indisulam (E7070) in combination with CPT-11 for cancer treatment. Cancer Chemother Pharmacol 2012; 69: 1353-1362.

[11] Ting TC, Goralski M, Klein K, Wang B, Kim J, Xie Y and Nijhawan D. Aryl sulfonamides degrade RBM39 and RBM23 by recruitment to CRL4-DCAF15. Cell Rep 2019; 29: 1499-1510, e6.

[12] Voss PG and Wang JL. Liquid-liquid phase separation: Galectin-3 in nuclear speckles and ribonucleoprotein complexes. Exp Cell Res 2023; 427: 113571.

[13] Han T, Goralski M, Gaskill N, Capota E, Kim J, Ting TC, Xie Y, Williams NS and Nijhawan D. Anticancer sulfonamides target splicing by inducing RBM39 degradation via recruitment to DCAF15. Science 2017; 356: eaal3755.

[14] Uehara T, Minoshima Y, Sagane K, Sugi NH, Mitsuhashi KO, Yamamoto N, Kamiyama H, Takahashi K, Kotake Y, Uesugi M, Yokoi A, Inoue A, Yoshida T, Mabuchi M, Tanaka A and Owa T. Selective degradation of splicing factor CAPERα by anticancer sulfonamides. Nat Chem Biol 2017; 13: 675-680.

[15] Bussiere DE, Xie L, Srinivas H, Shu W, Burke A, Be C, Zhao J, Godbole A, King D, Karki RG, Hornak V, Xu F, Cobb J, Carte N, Frank AO, Frommlet A, Graff P, Knapp M, Fazal A, Okram B, Jiang S, Michellys PY, Beckwith R, Voshol H, Wiesmann C, Solomon JM and Paulk J. Structural basis of indisulam-mediated RBM39 recruitment to DCAF15 E3 ligase complex. Nat Chem Biol 2020; 16: 15-23.

[16] Xu Y, Nijhuis A and Keun HC. RNA-binding motif protein 39 (RBM39): an emerging cancer target. Br J Pharmacol 2022; 179: 2795-2812.

[17] Kumar PP, Emechebe U, Smith R, Franklin S, Moore B, Yandell M, Lessnick SL and Moon AM. Coordinated control of senescence by lncRNA and a novel T-box3 co-repressor complex. Elife 2014; 3: e02805.

[18] Mai S, Qu X, Li P, Ma Q, Cao C and Liu X. Global regulation of alternative RNA splicing by the SR-rich protein RBM39. Biochim Biophys Acta 2016; 1859: 1014-1024.

[19] Kotake Y, Sagane K, Owa T, Mimori-Kiyosue Y, Shimizu H, Uesugi M, Ishihama Y, Iwata M and Mizui Y. Splicing factor SF3b as a target of the antitumor natural product pladienolide. Nat Chem Biol 2007; 3: 570-575.

[20] O'Keefe RT, Mayeda A, Sadowski CL, Krainer AR and Spector DL. Disruption of pre-mRNA splicing in vivo results in reorganization of splicing factors. J Cell Biol 1994; 124: 249-260.

[21] Rossi M, Sayan AE, Terrinoni A, Melino G and Knight RA. Mechanism of induction of apoptosis by p73 and its relevance to neuroblastoma biology. Ann N Y Acad Sci 2004; 1028: 143-149.

[22] Liu PF, Hu YC, Kang BH, Tseng YK, Wu PC, Liang CC, Hou YY, Fu TY, Liou HH, Hsieh IC, Ger LP and Shu CW. Expression levels of cleaved caspase-3 and caspase-3 in tumorigenesis and prognosis of oral tongue squamous cell carcinoma. PLoS One 2017; 12: e0180620.

[23] O'Donovan N, Crown J, Stunell H, Hill AD, McDermott E, O'Higgins N and Duffy MJ. Caspase 3 in breast cancer. Clin Cancer Res 2003; 9: 738-742.

[24] Silva FFVE, Padín-Iruegas ME, Caponio VCA, Lorenzo-Pouso AI, Saavedra-Nieves P, Chamorro-Petronacci CM, Suaréz-Peñaranda J and Pérez-Sayáns M. Caspase 3 and cleaved caspase 3 expression in tumorogenesis and its correlations with prognosis in head and neck cancer: a systematic review and meta-analysis. Int J Mol Sci 2022; 23: 11937.

[25] Yoshino H, Ueda N, Niijima J, Sugumi H, Kotake Y, Koyanagi N, Yoshimatsu K, Asada M, Watanabe T, Nagasu T, et al. Novel sulfonamides as potential, systemically active antitumor agents. J Med Chem 1992; 35: 2496-2497.
[26] Fukuoka K, Usuda J, Iwamoto Y, Fukumoto H, Nakamura T, Yoneda T, Narita N, Saijo N and Nishio K. Mechanisms of action of the novel sulfonamide anticancer agent E7070 on cell cycle progression in human non-small cell lung cancer cells. Invest New Drugs 2001; 19: 219-227.
[27] Nijhuis A, Sikka A, Yogev O, Herendi L, Balcells C, Ma Y, Poon E, Eckold C, Valbuena GN, Xu Y, Liu Y, da Costa BM, Gruet M, Wickremesinghe C, Benito A, Kramer H, Montoya A, Carling D, Want EJ, Jamin Y, Chesler L and Keun HC. Indisulam targets RNA splicing and metabolism to serve as a therapeutic strategy for high-risk neuroblastoma. Nat Commun 2022; 13: 1380.
[28] Singh S, Quarni W, Goralski M, Wan S, Jin H, Van de Velde LA, Fang J, Wu Q, Abu-Zaid A, Wang T, Singh R, Craft D, Fan Y, Confer T, Johnson M, Akers WJ, Wang R, Murray PJ, Thomas PG, Nijhawan D, Davidoff AM and Yang J. Targeting the spliceosome through RBM39 degradation results in exceptional responses in high-risk neuroblastoma models. Sci Adv 2021; 7: eabj5405.
[29] Wang E, Lu SX, Pastore A, Chen X, Imig J, Chun-Wei Lee S, Hockemeyer K, Ghebrechristos YE, Yoshimi A, Inoue D, Ki M, Cho H, Bitner L, Kloetgen A, Lin KT, Uehara T, Owa T, Tibes R, Krainer AR, Abdel-Wahab O and Aifantis I. Targeting an RNA-binding protein network in acute myeloid leukemia. Cancer Cell 2019; 35: 369-384, e7.
[30] Wang ET, Sandberg R, Luo S, Khrebtukova I, Zhang L, Mayr C, Kingsmore SF, Schroth GP and Burge CB. Alternative isoform regulation in human tissue transcriptomes. Nature 2008; 456: 470-476.
[31] Keren H, Lev-Maor G and Ast G. Alternative splicing and evolution: diversification, exon definition and function. Nat Rev Genet 2010; 11: 345-355.
[32] Climente-González H, Porta-Pardo E, Godzik A and Eyras E. The functional impact of alternative splicing in cancer. Cell Rep 2017; 20: 2215-2226.
[33] Urbanski LM, Leclair N and Anczuków O. Alternative-splicing defects in cancer: splicing regulators and their downstream targets, guiding the way to novel cancer therapeutics. Wiley Interdiscip Rev RNA 2018; 9: e1476.
[34] Lee SC and Abdel-Wahab O. Therapeutic targeting of splicing in cancer. Nat Med 2016; 22: 976-986.
[35] Carneiro BA and El-Deiry WS. Targeting apoptosis in cancer therapy. Nat Rev Clin Oncol 2020; 17: 395-417.
[36] Goldar S, Khaniani MS, Derakhshan SM and Baradaran B. Molecular mechanisms of apoptosis and roles in cancer development and treatment. Asian Pac J Cancer Prev 2015; 16: 2129-2144.
[37] Bock FJ and Tait SWG. Mitochondria as multifaceted regulators of cell death. Nat Rev Mol Cell Biol 2020; 21: 85-100.
[38] Kiraz Y, Adan A, Kartal Yandim M and Baran Y. Major apoptotic mechanisms and genes involved in apoptosis. Tumour Biol 2016; 37: 8471-8486.
[39] Ramos H, Raimundo L and Saraiva L. p73: from the p53 shadow to a major pharmacological target in anticancer therapy. Pharmacol Res 2020; 162: 105245.
[40] Zhang Q, Di C, Yan J, Wang F, Qu T, Wang Y, Chen Y, Zhang X, Liu Y, Yang H and Zhang H. Inhibition of SF3b1 by pladienolide B evokes cycle arrest, apoptosis induction and p73 splicing in human cervical carcinoma cells. Artif Cells Nanomed Biotechnol 2019; 47: 1273-1280.
[41] Vikhreva P, Melino G and Amelio I. p73 alternative splicing: exploring a biological role for the C-terminal isoforms. J Mol Biol 2018; 430: 1829-1838.
[42] Omran Z, H Dalhat M, Abdullah O, Kaleem M, Hosawi S, A Al-Abbasi F, Wu W, Choudhry H and Alhosin M. Targeting post-translational modifications of the p73 protein: a promising therapeutic strategy for tumors. Cancers (Basel) 2021; 13: 1916.

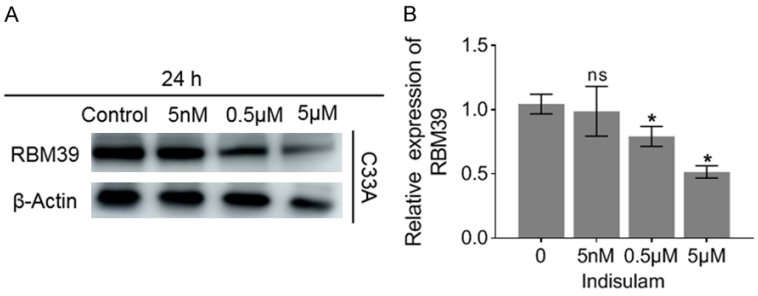

Supplementary Figure 1. Indisulam treatment induces RBM39 degradation of C33A cells. Western blot of C33A cells treated with 0, 5 nM, 0.5 μM or 5 μM indisulam for 24 h. Data represent the mean ± SD of three independent experiments each conducted in triplicate. ns: no significant difference, **P*<0.05 (one-way ANOVA).